AD-A143 935 STRUCTURE AND PROPERTIES OF POLYMERS AND ORGANOSILANES ABSORBED ONTO OXID.. (U) CINCINNATI UNIV OH DEPT OF MATERIALS SCIENCE AND METALLURGICA.. F J BOERIO

1/1

UNCLASSIFIED 15 JUL 84 N00044-80-C-0733 F/G 11/1 NL

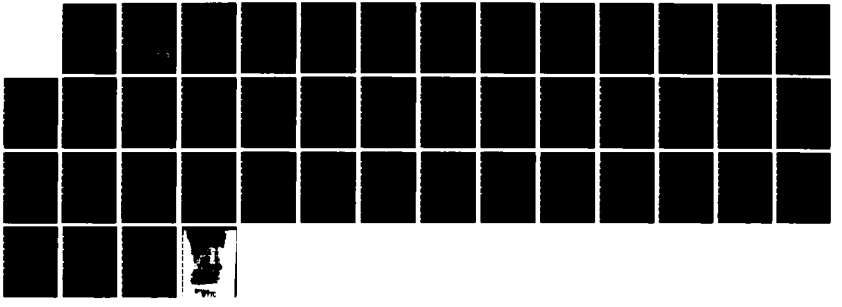

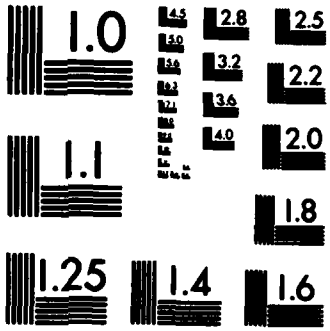

(12)

Annual Report No. 4
Contract N00014-80-C-0733; NR-039-202

Structure and Properties of Polymers and Organosilanes Adsorbed Onto Oxidized Aluminum and Titanium

F. James Boerio
Department of Materials Science
and Metallurgical Engineering
University of Cincinnati
Cincinnati, Ohio 45221-0012

July 15, 1984

Interim Report for Period July 1, 1983 to June 30, 1984

Prepared for:

Office of Naval Research
800 North Quincy Street
Arlington, VA 22217

SECURITY CLASSIFICATION OF THIS PAGE (When Data Entered)

REPORT DOCUMENTATION PAGE	READ INSTRUCTIONS BEFORE COMPLETING FORM
1. REPORT NUMBER: Annual Report No. 4	2. GOVT ACCESSION NO.: AD-A143935
	3. RECIPIENT'S CATALOG NUMBER
4. TITLE (and Subtitle): Structure and Properties of Polymers and Organosilanes Adsorbed Onto Oxidized Aluminum and Titanium	5. TYPE OF REPORT & PERIOD COVERED: Interim July 1, 1983 - June 30, 1984
	6. PERFORMING ORG. REPORT NUMBER
7. AUTHOR(s): F. James Boerio	8. CONTRACT OR GRANT NUMBER(s): N00014-80-C-0733
9. PERFORMING ORGANIZATION NAME AND ADDRESS: Department of Materials Science, University of Cincinnati, Cincinnati, Ohio 45221-0012	10. PROGRAM ELEMENT, PROJECT, TASK AREA & WORK UNIT NUMBERS: Work Unit No. NR-039-202
11. CONTROLLING OFFICE NAME AND ADDRESS: Office of Naval Research, 800 N. Quincy Street, Arlington, Virginia 22217	12. REPORT DATE: July 15, 1984
	13. NUMBER OF PAGES: 43
14. MONITORING AGENCY NAME & ADDRESS (if different from Controlling Office)	15. SECURITY CLASS. (of this report)
	15a. DECLASSIFICATION/DOWNGRADING SCHEDULE

16. DISTRIBUTION STATEMENT (of this Report)

Unlimited

DISTRIBUTION STATEMENT A
Approved for public release
Distribution Unlimited

17. DISTRIBUTION STATEMENT (of the abstract entered in Block 20, if different from Report)

Unlimited

DISTRIBUTION STATEMENT A
Approved for public release
Distribution Unlimited

18. SUPPLEMENTARY NOTES

19. KEY WORDS (Continue on reverse side if necessary and identify by block number)

Metal-to-Metal Adhesive Bonds
Organosilane Primers
Hydrothermal Stability of Adhesive Bonds
X-Ray Photoelectron Spectroscopy
Aluminum
Titanium
Iron

20. ABSTRACT (Continue on reverse side if necessary and identify by block number)

X-ray photoelectron spectroscopy (XPS) was used to determine the locus of failure in iron/epoxy lap joints that had been immersed in water at 60°C for long times and then tested to determine their retained strength. The fracture surfaces of joints prepared from adherends pretreated with aqueous solutions of γ-aminopropyltriethoxysilane (γ-APS) at pH 8.0 contained significant amounts of silicon but very little iron, indicating

DD FORM 1 JAN 73 1473 EDITION OF 1 NOV 65 IS OBSOLETE
S/N 0102-LF-014-6601

SECURITY CLASSIFICATION OF THIS PAGE (When Data Entered)

that failure was probably near the adhesive/silane interface. Fracture surfaces of joints prepared from unprimed adherends or adherends primed with aqueous solutions of γ-APS at pH 10.4 contained a great deal of iron, indicating that failure was near the oxide surface.

Results obtained from XPS indicated that there was a difference in the orientation of γ-APS molecules adsorbed onto iron from aqeuous solutions at pH 8.0 and 10.4. The surfaces of films formed at pH 8.0 contained significantly more oxygen than those formed at pH 10.4. The oxygen on the surfaces of films formed at pH 8.0 was mostly in a siloxane form. Oxygen on the surfaces of films formed at pH 10.4 was mostly in a hydroxyl form. The variation in performance of γ-APS primers as a function of pH are undoubtedly related to these structural differences.

The acid-base characteristics of polished titanium, iron, and zinc mirrors were estimated using indicators. The isoelectric points of the oxidized surfaces were estimated as 4.1, 7.3, and 9.2, respectively.

The time to failure for statically loaded aluminum/epoxy tapered double cantilever beams exposed to water at 60°C was significantly increased by the use of γ-APS primers. The increase in time to failure was greater for large loads than for small loads, perhaps indicating a difference in failure mechanisms for different loading conditions.

I. Introduction

One of the most important limitations regarding the use of adhesive bonding for joining metals concerns the adverse effects of water. In the absence of water, properly prepared adhesive joints are very strong. The failure of such joints is almost invariably cohesive within the adhesive. However, in the presence of moisture even the most carefully prepared adhesive joints weaken and eventually fail near the interface.

The adverse effects of moisture are not unique to metal-to-metal adhesive joints. A very similar problem is encountered in glass fiber reinforced composites. In that case the solution to the problem has been to pretreat the glass fibers with dilute aqueous solutions of organosilane "coupling agents" (1). The primary objective of this research is to determine the applicability of organosilanes as "primers" for improving the hydrothermal stability of metal-to-metal adhesive joints.

Several theories have been suggested to describe the mechanisms by which silanes function as coupling agents on glass fibers (1). Perhaps the most widely accepted is the so-called chemical bonding theory (see Figure 1). This theory envisions that silane coupling agents function by forming stable covalent bonds with both the substrate and an adhesive applied to the substrate. However, little direct evidence to support this theory has been reported in the past. An additional objective of this research is to determine the mechanisms by which organosilanes interact with the oxidized surfaces of metals and

improve the hydrothermal stability of metal-to-metal adhesive joints.

The usefulness of organofunctional silanes as primers for enhancing the hydrothermal stability of metal-to-metal adhesive joints was determined in several ways. In some cases metal/epoxy lap joints were immersed in water at 60°C and the strength retained was determined as a function of immersion time. In other cases, the time required for a preexisting crack to extend the entire length of statically loaded, tapered double cantilever beams during immersion in water at 60°C was determined. The mechanisms by which silanes function as primers were determined using surface analysis techniques such as reflection-absorption infrared spectroscopy (RAIR), ellipsometry, and x-ray photoelectron spectroscopy (XPS) to determine the structure of thin films formed by silanes adsorbed onto metal mirrors from dilute aqueous solutions and to determine the locus of failure of adhesive joints that had been exposed to water for long periods of time.

Previous reports have described the molecular structure of thin films of γ-aminopropyltriethoxysilane (γ-APS) adsorbed onto iron, titanium, and aluminum and the properties of such films as primers for improving the wet strength of iron/epoxy, titanium/epoxy, and aluminum/epoxy adhesive joints. This report describes some additional features of the structure of γ-APS primer films on iron, titanium, and aluminum and discusses the mechanisms by which such films improve the hydrothermal stability of iron/epoxy, titanium/epoxy, and aluminum/epoxy adhesive joints.

II. Experimental

Iron/epoxy lap joints were prepared according to ASTM Standard D1002. Iron adherends (1 x 4 x 0.063") were mechanically polished, rinsed repeatedly, and dried in nitrogen. Pairs of adherends were then bonded together using an adhesive consisting of an epoxy resin (Epon 828, Shell Chemical Company) and 9.4 weight percent of a tertiary amine catalyst (Ancamine K-61B, Pacific Anchor Chemical Company or Shell Curing Agent D, Shell Chemical Company). The adhesive was cured by heating in an oven at 110°C for one hour. Primer films were applied to some of the adherends by immersing them in 1% aqueous solutions of γ-aminopropyltriethoxysilane (A-1100, Union Carbide Corporation) for appropriate times, removing the adherends from the solution, and blowing the excess solution off the adherends using a strong stream of nitrogen. In other cases the adherends were left unprimed as a control. In all cases the lap joints were immersed in water at 60°C. At various intervals, joints were removed from the water, dried, and tested using an Instron Universal Testing Instrument to determine the breaking strength.

Aluminum/epoxy tapered double cantilever beams were prepared as described by Mostovoy and Ripling (2) and as shown in Figure 2. 2024-T3 aluminum adherends were mechanically polished, rinsed, and dried. Some of the adherends were then primed by flooding the surfaces with 1% aqueous solutions of γ-APS. After ten minutes the excess solution was blown off the adherends using a strong stream of nitrogen. Pairs of adherends were then bonded together using the same adhesive and curing schedule as described

above. Aluminum shims near each end of the beams were used to control the thickness of the bondline at 0.5 mm. Increasing loads were applied to the beams using the Instron and a strain rate of 0.05 inches/minute. Static loads were applied using an apparatus that was originally designed for creep testing of metals. The displacement of the beams (δ in Figure 2) was measured using a linear variable differential transformer (LVDT) and recorded using a microcomputer. The crack length (c in Figure 2) was related to δ and to P, the load applied to the beams, using the expression

$$\Delta C \text{ (in)} = \Delta\delta \text{ (in)} \times 10^4/1.44 \text{ P (lbs)}$$

which was developed by Mostovoy for the TDCB configuration (2).

Samples for x-ray photoelectron spectroscopy were prepared using mechanically polished iron mirrors as substrates. Freshly polished mirrors were immersed in 1% aqueous solutions of γ-APS for a few minutes, rinsed in water, and dried. XPS spectra were obtained using Physical Electronics x-ray photoelectron spectrometers. In all cases, magnesium K_α radiation was used to excite the photoelectron spectra. When a Physical Electronics Model 5300 spectrometer was used, nondestructive depth profiling was done using a technique known as angle-resolved XPS. In angle-resolved XPS, the sampling depth varies as the sample is tilted to change the angle between the sample surface and the beam of photoelectrons exiting from the surface. When this "exit angle" is small, the sampling depth is small (only a few atomic layers). When the exit angle is large, the sampling depth is relatively large (a few tens of angstroms).

III. Results and Discussion

A. Hydrothermal Stability of Iron/Epoxy Lap Joints.

We have previously shown that γ-aminopropyltriethoxysilane (γ-APS) is most effective as a primer for enhancing the hydrothermal stability of iron/epoxy lap joints when the silane is applied to the adherends from acidified aqueous solutions (3,4). That result has been confirmed for a new set of lap joints. As shown in Figure 3, the strength of all of the iron/epoxy lap joints decreased rapidly during the first 15 days of immersion in water at 60°C. After 15 days the strength of the joints continued to decrease but at a much slower rate. After 40 days, joints prepared from unprimed adherends retained about 20% of their initial strength. Joints prepared from adherends primed with γ-APS at pH 10.4 retained about 35% of their initial strength. Joints prepared from adherends primed with γ-APS at pH 8.0 were most durable and retained about 60% of their initial strength after immersion for 40 days in water at 60°C.

The fracture surfaces of iron/epoxy lap joints that had been tested after lengthy immersion in water at 60°C were examined using scanning electron microscopy (SEM) and x-ray photoelectron spectroscopy (XPS) in order to determine the locus of failure. Results obtained from SEM indicated that failure of the joints was always close to the adhesive/adherend interface. However, some adhesive was always observed on the fracture surfaces of adherends that had been primed with γ-APS at pH 8.0 prior to bonding. Little adhesive was observed on the fracture surfaces of adherends that had not been primed or else had been primed at

pH 10.4 before bonding. This was especially the case after longer immersion times.

Results obtained from XPS provided more information regarding the locus of failure of the iron/epoxy lap joints that were tested after immersion in water at 60°C. The Fe(2p) spectra obtained from the adherend surfaces of joints that were fractured after immersion for seven days are shown in Figure 4. Intense Fe(2p) spectra were obtained from adherends that were either not primed or were primed with γ-APS at pH 10.4 prior to bonding. Only weak Fe(2p) spectra were obtained from adherends primed at pH 8.0 and then bonded.

The Fe(3s) and Si(2p) spectra obtained from the same fracture surfaces are shown in Figure 5. The Fe(3s) spectra were observed near 100.5 and 94.0 eV for the unprimed adherend but the Si(2p) spectra, which are normally observed near 103.0 eV for siloxane polymers, were not observed. The fracture surface of the adherend primed at pH 10.4 was characterized by an Fe(3s) peak near 94.0 eV and by a weak Si(2p) peak near 102.5 eV that was superimposed on the Fe(3s) peak near 101.0 eV. The fracture surface of the adherend primed at pH 8.0 was characterized by a relatively strong Si(2p) peak near 103.5 eV.

The O(1s) spectra obtained from the fracture surfaces are shown in Figure 6. The spectra from unprimed adherends were characterized by a band near 530.5 eV that is typical of iron oxides (5). Spectra obtained from adherends that were primed at pH 10.4 before bonding were quite similar. However, the O(1s) spectra obtained from adherends primed at pH 8.0 prior to bonding

were characterized by a strong band near 533.0 eV, that was assigned to a siloxane polymer, and by a weak shoulder near 530.0 eV that was assigned to the oxide.

The results obtained from XPS support the conclusion that joints prepared from adherends primed with γ-APS at pH 8.0 prior to bonding tended to fail within the primer when tested after immersion in water at 60°C for long times. The fracture surfaces of such joints were characterized by the presence of thin films of polymerized γ-APS and by the absence of iron. By comparison, joints prepared from unprimed adherends or from adherends primed with γ-APS at pH 10.4 tended to fail near the primer/oxide interface when tested after immersion for long times in water at 60°C. The fracture surfaces of those joints were characterized by only small amounts of adhesive or primer and by large amounts of iron oxides and hydroxides.

The results described above have confirmed that γ-APS is much more effective as a primer for improving the wet strength of iron/epoxy adhesive joints when applied to the adherends at pH 8.0 than when applied at pH 10.4. We have previously proposed a model that suggests γ-APS is more effective at pH 8.0 than at pH 10.4 because of an orientation effect (4). According to the model, the isoelectric point of the oxidized surface of iron is near 10.0 and the pK_a's of the amino and silanol groups on γ-APS are near 10.0 and 3.0, respectively. When γ-APS is adsorbed onto iron from an aqueous solution at pH 10.4, the oxide should have positive and negative sites but little net charge. The silanol groups should be ionized (as silanolate ions, SiO^-) and the amino

groups should be about half protonated (as NH_3^+) and half free (as NH_2).

Therefore, at pH 10.4, γ-APS should tend to adsorb onto the oxidized surface of iron through both the amino and silanol groups. When γ-APS is adsorbed onto iron from aqueous solutions at pH 8.0, the oxide should be positively charged. The amino groups should be mostly protonated (as NH_3^+) and the silanol groups should be mostly ionized (as SiO^-). Therefore, at pH 8.0, γ-APS should tend to adsorb onto the oxidized surface of iron through the silanol groups. Adsorption of γ-APS onto the oxidized surface of iron through the silanol groups was considered to be more stable in the presence of water than adsorption through the amino groups.

We have now used XPS to determine the structural differences in monomolecular films of γ-APS adsorbed onto the oxidized surface of iron from aqueous solutions at pH 8.0 and 10.4. The results are described below.

B. X-ray Photoelectron Spectroscopy of Monomolecular Films of γ-APS Adsorbed Onto Iron From Aqueous Solutions.

When XPS survey spectra were obtained from mechanically polished but unsilanated iron mirrors, the only elements detected were iron, carbon, and oxygen. The carbon was attributed to adsorbed hydrocarbon contaminants. The Fe(2p) and O(1s) spectra are shown in Figures 7 and 8, respectively. The $Fe(2p_{3/2})$ peak was observed near 711.0 eV, indicating that mostly Fe(III) was present in the oxide and that the oxide was mostly Fe_2O_3 (5). When the exit angle was 90° and photoelectrons from relatively

deep (~50Å) within the surface regions were detected, an additional Fe($2p_{3/2}$) peak characteristic of Fe(0) was observed near 706.8 eV. This peak was not observed when the exit angle was 10° and only photoelectrons from the outermost atomic layers (~10Å) were detected.

The structure of the O(1s) spectra for the polished iron was complex (see Figure 8). When the exit angle was 90°, a sharp peak was observed near 530.0 eV with a broad shoulder at higher binding energies. When the exit angle was 10°, the high energy shoulder became a well resolved band near 531.8 eV. In fact, as shown in Figure 9, the O(1s) spectra obtained from iron mirrors at an exit angle of 10° could be resolved into three components near 530.0, 531.8, and 533.3 eV. The O(1s) peaks near 530.0 and 531.8 eV were easily assigned to the oxide and to a surface hydroxide, respectively (5). The origin of the high energy component near 533.3 eV is not known at this time.

Next, an approximately monomolecular film of γ-APS was adsorbed onto a polished iron mirror by immersing the mirror in a 1% aqueous solution at pH 10.4 for 30 minutes. After that time, the mirror was removed from the solution, immediately rinsed in water, and dried. The elements iron, carbon, oxygen, silicon, and nitrogen were observed in XPS survey spectra obtained from such mirrors. The composition of the surface of one such sample is shown in Tables I and II for exit angles of 90° and 10°, respectively.

The Fe(2p) spectra obtained from these mirrors were essentially the same as those obtained from bare iron mirrors

Table I

Atomic Concentration of γ-APS Films Adsorbed Onto Iron From Aqueous Solutions at pH 10.4. The Exit Angle was 90°.

Element	Percent
Fe	11.53
O	57.38
C	22.94
N	3.36
Si	4.00

Table II

Atomic Concentration of γ-APS Films Adsorbed Onto Iron From Aqueous Solutions at pH 10.4. The Exit Angle was 10°.

Element	Percent
Fe	3.18
O	35.77
C	49.76
N	5.31
Si	5.98

(see Figure 7). The Si(2p) spectra showed an interesting dependence on exit angles (see Figure 10). When the exit angle was 90°, the Si(2p) peak near 102.5 eV had nearly the same intensity as the neighboring Fe(3s) band near 94.0 eV. However, when the exit angle was 10°, emphasizing the outermost atomic layers of the surface, the Si(2p) peak was much stronger than the Fe(3s) peak.

The O(1s) spectra for γ-APS films adsorbed onto iron at pH 10.4 are shown in Figure 11. For an exit angle of 90°, a peak characteristic of the oxide was observed near 530.0 eV and a broad shoulder was observed at higher binding energies. When the exit angle was 10°, a broad band was observed near 531.8 eV and the oxide band near 530.0 eV was observed as a shoulder. In fact, the O(1s) spectra obtained for an exit angle of 10° could be resolved into five components near 530.0, 531.1, 531.8, 532.2, and 533.3 eV (see Figure 12). That is, the O(1s) spectra for γ-APS adsorbed onto iron at pH 10.4 consisted of three bands that were observed for bare, unsilanated iron (530.0, 531.8, and 533.3 eV) and two new bands (531.1 and 532.2 eV). The origin of the new band near 531.1 eV is not known at present but it is felt that the band near 532.2 eV is characteristic of siloxane bonds.

The N(1s) spectra observed for γ-APS films adsorbed onto iron mirrors at pH 10.4 were resolved into components near 400.0 and 401.8 eV (see Figure 13). It is felt that these bands are related to free and protonated amino groups, respectively.

Finally, an approximately monomolecular film of γ-APS was adsorbed onto a polished iron mirror by immersing the mirror in a

1% aqueous solution at pH 8.0 for 30 minutes. After that time, the mirror was removed, rinsed in water, and dried. Once again the elements iron, carbon, nitrogen, oxygen, and silicon were observed in the XPS survey spectra. The composition of the surface of such a sample is shown in Tables III and IV for exit angles of 90° and 10°, respectively.

Comparing Tables III and IV with Tables I and II indicates that iron mirrors treated with γ-APS at pH 8.0 contain more oxygen and iron and less nitrogen and silicon in their surface regions than mirrors treated with γ-APS at pH 10.4. Comparing Tables II and IV emphasizes that the topmost layers of γ-APS films adsorbed onto iron at pH 8.0 are richer in oxygen than the topmost layers of films adsorbed at pH 10.4.

The Fe(2p) spectra for mirrors treated with γ-APS at pH 8.0 were very similar to the Fe(2p) spectra of bare iron (see Figure 7) and the Si(2p) and N(1s) spectra were very similar to the corresponding spectra for iron mirrors treated with γ-APS at pH 10.4 (see Figures 10 and 13). The most important difference in the XPS spectra of iron mirrors treated with γ-APS at pH 8.0 and pH 10.4 was observed in the O(1s) spectra (see Figure 14). When the exit angle was 90°, a sharp band was observed near 530.1 eV with a broad, unresolved shoulder extending to higher binding energies. When the exit angle was 10°, a strong, broad band was observed centered near 532.2 eV with a moderately strong shoulder near 530.1 eV. As indicated above, the band near 530.1 eV may be assigned to oxygen in the oxide lattice. The broad band centered near 532.2 eV probably contains several

Table III

Atomic Concentration of γ-APS Films Adsorbed Onto Iron From Aqueous Solutions at pH 8.0. The Exit Angle was 90°.

Element	Percent
Fe	14.21
O	61.72
C	17.97
N	2.34
Si	3.75

Table IV

Atomic Concentration of γ-APS Films Adsorbed Onto Iron From Aqueous Solutions at pH 8.0. The Exit Angle was 10°.

Element	Percent
Fe	3.24
O	45.38
C	42.09
N	3.84
Si	5.45

components. However, the position of this band indicates that oxygen atoms in siloxane bonds account for a great deal of its intensity.

Comparing Tables I and II with Tables III and IV indicates that iron mirrors treated with γ-APS at pH 8.0 have considerably more oxygen on the surface than mirrors treated with γ-APS at pH 10.4. This is especially the case when the exit angle is 10^{o}, emphasizing the composition of the outermost few atomic layers (see Tables II and IV). This conclusion is confirmed by comparing Figures 11b and 14b.

The type of oxygen observed on the surfaces of γ-APS films adsorbed onto iron mirrors at pH 8.0 and 10.4 is also different. When γ-APS is adsorbed onto iron at pH 10.4, the topmost atomic layers contain less oxygen and the oxygen is mostly in the oxide and in hydroxyl groups.

We are continuing to investigate the XPS spectra of monomolecular films of γ-APS adsorbed onto iron. However, the XPS experiments described above have been carried out twice and the results were very similar. Therefore, we have tentatively concluded that γ-APS molecules do orient differently when adsorbed onto iron mirrors from aqueous solutions at pH 8.0 and 10.4. There is a strong tendency for molecules adsorbed at pH 8.0 to orient with oxygen atoms toward the free surface. This effect is much weaker for molecules adsorbed at pH 10.4.

C. Isoelectric Points of Oxidized Surfaces of Metals.

In order to evaluate almost any theory of adhesive bonding, including the one described above for iron/epoxy joints using

γ-APS primers, it is important to determine the acid/base characteristics of the oxidized surfaces of the metal adherends. The acid/base nature of the surface can be described in terms of the isoelectric point of the surface (IEPS).

The surface of any metal adherend is, of course, covered with an oxide layer. However, as was shown above for iron adherends, the oxide itself is covered with a thin layer of hydroxide. In the presence of water, the hydroxyl groups on the surface of an oxide can be ionized. At high pH values the reaction

$$MOH + OH^- \rightleftarrows MO^- + H_2O$$

can occur while at low pH values the reaction

$$MOH + H^+ \rightleftarrows MOH_2^+$$

is obtained. At some intermediate value of pH referred to as the isoelectric point of the surface, the number of positive and negative charges on the surface are equal and there is no net charge on the surface. Hydroxides with low ISEP are acidic while those with high ISEP are basic. Parks (6) has shown that there is a correlation between valence and ISEP. Metals with low valences tend to have relatively high ISEP and metals with high valences have rather low ISEP.

Wightman (7) has shown that the ISEP of the oxidized surfaces of metal coupons can be estimated by observing color changes in aqueous solutions of indicators spread on the surfaces of the coupons. In particular, he showed that the ISEP of a titanium surface could be shifted by several pH units depending on pretreatment. We have used the same techniques to estimate

the ISEP of the oxidized surfaces of mechanically polished iron, titanium, and zinc mirrors. The indicators that were used and their approximate pK_a values are shown in Table V.

Indicator solutions were prepared by dissolving 0.01 grams of the indicators in 25 ml of water. Metal mirrors were mechanically polished, rinsed, and dried and a few drops of the indicator solutions were then spread over the surfaces of the mirrors. Visual color changes were observed for some of the solutions within a few minutes. The results obtained for titanium, iron, and zinc mirrors are summarized in Table VI.

No color change was observed when the indicator solutions were spread on titanium, implying that ISEP for this surface is rather low (<4.1). The indicators bromophenol blue and bromocresol green showed definite color changes on iron and bromothymol blue showed a weak change, indicating that ISEP for iron is near 7.3. All of the indicators except thymol blue and alizarin yellow changed color on zinc, indicating that ISEP for zinc is between 7.3 and 9.2.

These results indicate that the surface of the polished titanium mirrors is the most acidic and that the surface of zinc is the most basic. The surface of polished iron mirrors is intermediate. The present results are in qualitative agreement with values of ISEP given in the literature (8). For example, ISEP is frequently given as 6.0, 8.5 or 12.0, and 9.0 for titanium, iron, and zinc, respectively (8).

The two different values of ISEP given for iron, 8.5 and 12.0, refer to the Fe(III) and Fe(II) valence states,

Table V

pK_a's of Indicators Used to Estimate Isoelectric Points of Oxidized Metal Surfaces

Indicator	pK_a
Bromophenol Blue	4.1
Bromocresol Green	4.9
Bromothymol Blue	7.3
Thymol Blue	9.2
Alizarin Yellow	10-12

Table VI

Color Changes for Indicators Spread on Titanium, Iron, and Zinc

Indicator	pK_a	Color Change		
		Titanium	Iron	Zinc
Bromophenol Blue	4.1	RV→RV	RV→V	RV→BV
Bromocresol Green	4.9	Y→Y	Y→B	Y→B
Bromothymol Blue	7.3	Y→Y	Y→YB	Y→B
Thymol Blue	9.2	Y→Y	Y→Y	Y→Y
Alizarin Yellow	10-12	Y→Y	Y→Y	Y→Y

R - red, V- violet, Y- yellow, B- blue

respectively. The value obtained here for ISEP of iron (7.3) probably indicates that most of the iron on the surface of mechanically polished iron mirrors is in the Fe(III) state. This result is consistent with the XPS results described above. However, it should be emphasized that the XPS spectra do not exclude the possibility of some Fe(II) on the surface of iron mirrors exposed to the atmosphere.

D. Fracture of Aluminum/Epoxy Tapered Double Cantilever Beams.

Mostly we have used lap joints to determine the effects of organofunctional silanes on the wet strength of adhesive bonds to metals. However, there are a number of well known problems associated with the use of lap joints. The stress distribution in a lap joint is very dependent on geometry and is very uneven. The maximum shear stress is at the ends of the joint and can be several times greater than the average shear stress (9). As a result, the applicability of failure criteria based on the average shear stress in lap joints to other joint configurations is difficult to assess. Moreover, structural adhesives are usually brittle materials that fail by crack initiation and propagation rather than by yielding and flow (10). As a result, it is desirable to develop failure criteria based on fracture energy rather than average stress. However, it is very difficult to determine fracture energies for lap joints (11).

For these reasons we have determined G_c, refered to as the critical strain energy release rate and equivalent to the energy required to create a unit area of fracture surface by crack propagation, using the tapered double cantilever beam

configuration shown in Figure 2. This joint has the advantage that G_c is independent of crack length and is simply related to P_c, the applied load required to propagate a preexisting, stationary crack. The relation between G_c and P_c is

$$G_c = 4P_c^2 m/b^2 E$$

where b is the thickness of the beams, E is the elastic modulus of the adherend material, and m is a geometrical factor (2). The beams are contoured such that m, which is given by $(3c^2/h^3 + 1/h)$, equals 90 in^{-1}.

Actually, an adhesive joint can fail under a variety of conditions. Failure could result from application of a single, large load or from application of a small fixed load in an aggressive medium. Therefore, two separate cases were considered. In one, an increasing load was applied to the beams and P_c, the critical load causing propagation of a pre-crack, was determined. In the second case, a static load G_a, that was less than G_c, was applied to the beams during immersion in water at 60°C and the crack length was measured as a function of time. The results obtained so far are described below.

As indicated earlier, aluminum shims were located near each end of the TDCB specimens to control the bond thickness. The shim near the loading holes also served as a blunt pre-crack. When an increasing load was applied to a TDCB specimen that had been maintained at laboratory temperatures and humidities, the blunt pre-crack would suddenly jump forward along the center of the bond (COB) and then arrest. Thereafter, a G_c value of about 1.24×10^5 mj/m^2 was required to propagate the crack in a

somewhat unstable manner. The value of G_c required to propagate the crack did not depend on the pretreatment of the adherends and was considered to be a property of the adhesive.

In another series of experiments, TDCB specimens were pre-cracked by applying an increasing load. The specimens were then immersed in a water bath held at 60°C and statically loaded. In almost all cases, a long induction period ensued during which the initial COB pre-crack remained nearly stationary. During this time a new interfacial (IF) crack formed just above or below the tip of the starter crack. Eventually this new IF crack propagated at high speed, resulting in catastrophic failure of the beams.

The only exceptions to this behavior were observed for TDCB specimens prepared from unprimed adherends and loaded at G_a values that were close to the value of G_c for dry joints. In such cases an IF crack formed near the tip of the COB pre-crack and then propagated at a rate that increased with time. Examples of both types of crack propagation that were observed for statically loaded TDCB specimens immersed in water at 60°C are shown in Figure 15.

When the total time to failure was plotted against G_a, the results shown in Figure 16 were obtained. When the applied load was close to G_c, the total time to failure was much longer for specimens prepared from primed adherends than for those prepared from unprimed adherends and was related to the very long induction times that were observed for specimens prepared from primed adherends. When the applied load was much less than G_c,

the difference in total time to failure for primed and unprimed beams was less. However, the failure time was still greater for joints prepared from primed adherends. In all cases, the total time to failure was greater for beams prepared from adherends primed with γ-APS at pH 7.0 than for those primed at pH 10.4.

It is very interesting to compare the results obtained here with those obtained by others. Mostovoy and Ripling reported slow, steady interfacial crack growth in amine-cured (2) and anhydride-cured (12) aluminum/epoxy TDCB specimens that were statically loaded at $G_a<G_c$ and exposed to water or high relative humidities at room temperature. They also reported that there was a lower limit to the applied loads that would cause such slow interfacial crack growth in the presence of moisture (2,12). This limit was referred to as G_{scc} (for stress corrosion cracking) and it was suggested that interfacial crack growth would not occur for $G_a<G_{scc}$.

The results obtained here are more similar to those reported by Kinloch et al. (13). They observed an induction time prior to interfacial cracking for statically loaded aluminum/epoxy TDCB specimens exposed to water or high humidities at ambient temperatures. They also showed that an organofunctional silane, γ-glycidoxypropyltrimethoxysilane (γ-GPS), could be used as a primer to increase the total time to failure for the beam and that the increase was about the same for all applied loads (less than G_c, of course).

It is interesting to consider the reasons for the differences in the results obtained here and those reported by

Mostovoy (2) and by Kinloch (13). We used a tertiary amine curing agent (as did Kinloch) but Mostovoy used anhydride and amine curing agents. Tertiary amines cure epoxy resins catalytically, resulting in a network of ether bonds that is relatively resistant to hydrolysis. Anhydride curing agents result in the formation of ester bonds that are less resistant.

In the present case, the stress near the tip of the pre-crack was sufficient to cause an IF crack to form just above or below the tip of the pre-crack. However, the available strain energy was not sufficient to cause the IF crack to propagate. After prolonged exposure to water the interface was sufficiently weakened that the IF crack did propagate. At least in the case of anhydride curing agents, the interface is probably sufficiently susceptible to stress corrosion that IF cracks can form near the tip of the COB pre-crack and propagate without an induction period.

The results obtained so far indicate that γ-APS is more effective as a primer at larger applied loads (and shorter times to failure) than at smaller loads (and longer failure times). By comparison, Kinloch found that γ-GPS was equally effective at all applied loads (13). The reason for the difference is not known for certain but may be related to the temperature of the water that the beams were immersed in. Kinloch et al. (13) used water at ambient temperatures whereas water at 60^{o}C was used here. It may be that failure for large applied loads is related to hydrolysis at the oxide/primer or oxide/adhesive interface and that hydrolysis at the oxide/primer interface is slow. Failure

at small loads may be related to hydrolysis in the oxide and may not depend signficantly on the nature of the organic compounds adjacent to the oxide.

E. Effect of Residual Stresses on Failure of Adhesive Joints.

The results shown in Figure 16 indicate that static loads can have a significant effect on the time to failure for adhesive joints exposed to moisture at elevated temperatures. However, the results shown in Figure 3 indicate that the load carrying capability of joints can decrease during hydrothermal aging even in the absence of externally applied loads. It seems likely that residual stresses arising from cure shrinkage and differential thermal contraction may facilitate degradation of adhesive bonds during exposure to warm moist atmospheres.

We are investigating the effects of residual stresses using the double cantilever beam (DCB) configuration shown in Figure 17. DCB samples are prepared by casting an epoxy beam on top of a polished metal beam. The residual stress in the epoxy beam can be measured using photoelastic techniques. Residual stresses can be increased by curing the epoxy at elevated temperatures or decreased by curing the epoxy while the metal beam is under tension. A crack is initiated at the adhesive/adherend interface and the velocity of the crack is measured as a function of total stress (applied plus residual) during exposure to warm, moist atmospheres. External loads are applied to the beams through the loading holes shown in Figure 17. Crack velocities are measured using a cathetometer.

Preliminary results indicate that cracks will readily propagate along the adhesive/adherend interface when residual stresses are high but not when such stresses are low. We are continuing to investigate the effect of residual stresses on the hydrothermal stability of adhesive bonds. We are also investigating the effect of silane primers on residual stresses and on interfacial crack propagation in DCB specimens.

IV. Conclusions

The results obtained here confirm that γ-aminopropyltriethoxysilane (γ-APS) is an effective primer for increasing the hydrothermal stability of iron/epoxy adhesive bonds and that γ-APS is most effective when applied to iron adherends from aqueous solutions that have been acidified from pH 10.4 to pH 8.0. The locus of failure in iron/epoxy lap joints that were immersed in water at 60°C for long times and then tested to determine their retained strength was always near the interface. However, joints prepared from adherends primed at pH 8.0 failed near the adhesive/primer interface while joints prepared from adherends that were unprimed or primed with γ-APS at pH 10.4 failed near the oxide surface.

Monomolecular films formed by γ-APS adsorbed onto the oxidized surfaces of iron mirrors from aqueous solutions at pH 8.0 and pH 10.4 have different molecular orientations. The surface regions of films formed at pH 8.0 contain more oxygen than those formed at pH 10.4. Much of the oxygen on the surface of the films formed at pH 8.0 is in a siloxane form. The oxygen

on the surface of the films formed at pH 10.4 is mostly in a hydroxyl form. The structural differences in these films are related to the differences in durability observed for iron/epoxy lap joints prepared from adherends primed with γ-APS at pH 8.0 and 10.4.

The isoelastic points of titanium, iron, and zinc were estimated as 4.1, 7.3, and 9.2, respectively, using indicator dyes. The surfaces of iron and titanium were somewhat more acidic than previously thought.

The time to failure for statically loaded aluminum/epoxy tapered double cantilever beams immersed in water at 60°C was greatly increased by pretreating the adherends with dilute aqueous solutions of γ-APS, especially at relatively large loads. For small loads the effect of silane primers was reduced, perhaps indicating a change in the failure mechanism.

V. References

1. Plueddemann, E. P. and P. W. Erickson, in Composite Materials, vol. 6, L. J. Broutman and R. H. Krock, eds., Academic Press, New York (1974), Ch. 1.

2. Mostovoy, S. and E. J. Ripling, J. Appl. Polymer Sci. 13, 1083 (1969).

3. Boerio, F. J. and J. W. Williams, Appl. Surf. Sci. 7, 19 (1981).

4. Boerio, F. J., and R. G. Dillingham, in Proc. Intl. Symp. on Adhesive Joints: Formation, Characteristics, and Testing, K. L. Mittal, ed., to be published, 1984.

5. Brundle, C. R., Chuang, T. J., and K. Wandelt, Surf. Sci. 68, 459 (1977).

6. Parks, G. A., Chem. Rev. 65, 177 (1965).

7. Mason, J. G., Siriwardane, R., and J. P. Wightman, J. Adhesion 11, 315 (1981).

8. Pluddemann, E. P., Silane Coupling Agents, Plenum Press (New York), 1982, p. 91.

9. Adams, R. D., and N. A. Peppiatt, J. Strain Anal. 8, 134 (1973).

10. Bascom, W. D., Cottington, R. L., and C. O. Timmons, Appl. Polymer Symp. 32, 165 (1977).

11. DeVries, K. L., Williams, M. L., and M. D. Chang, Exp. Mech. 14, 89 (1974).

12. Mostovoy, S., and E. J. Ripling, J. Appl. Polymer Sci. 15, 641 (1971).

13. Kinloch, A. J., Dukes, W. A., and R. A. Gledhill, in Polymer Science and Technology, vol. 9B, L. H. Lee, ed., Plenum Press (New York), 1975, p. 597.

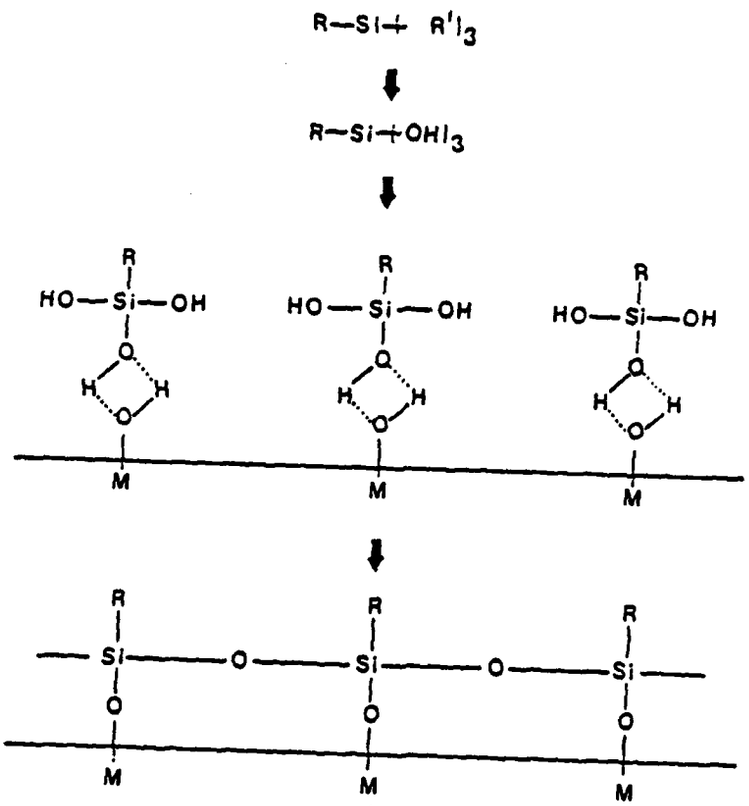

Figure 1. Chemical bonding theory of mechanism by which silane "Coupling agents" function.

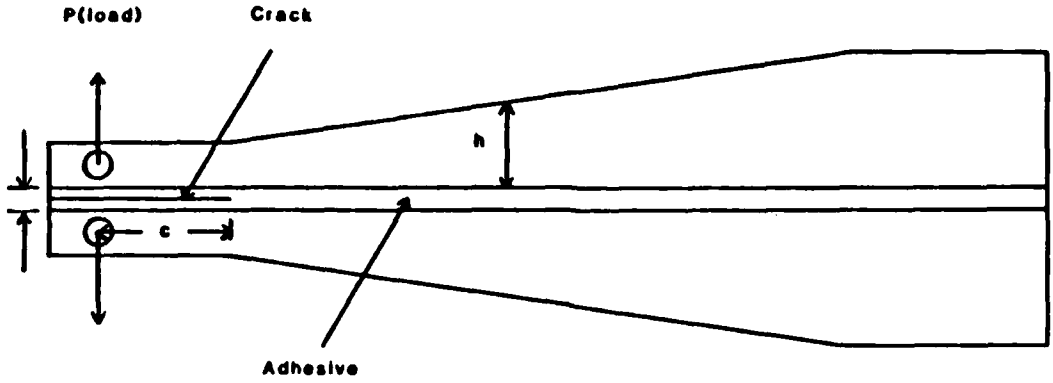

Figure 2. Tapered double cantilever beam specimen for determining fracture energy of adhesive joints.

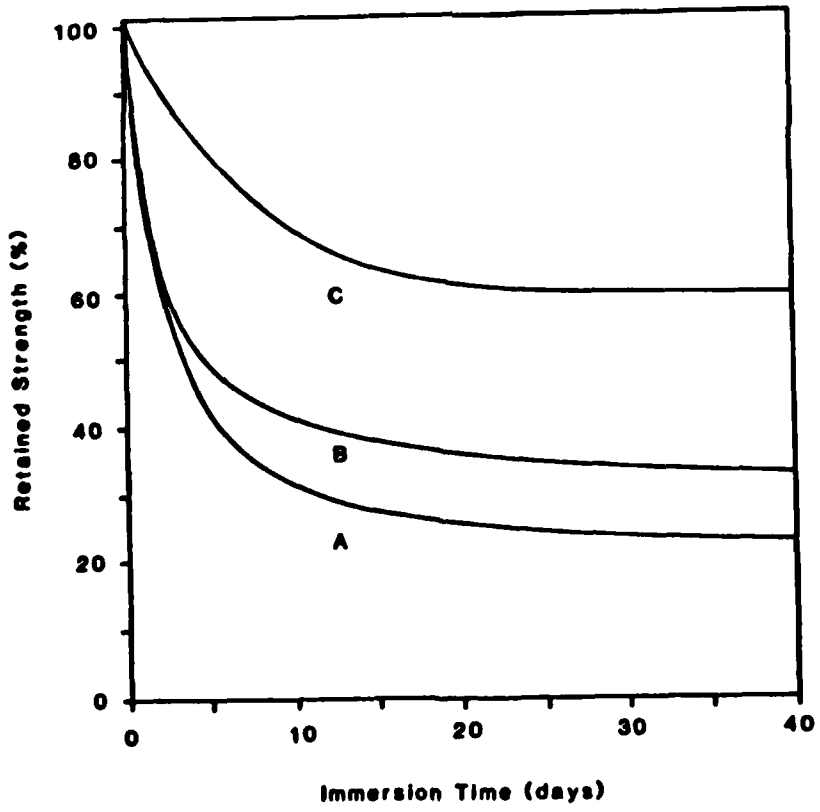

Figure 3. Breaking strength versus immersion time for iron/epoxy lap joints immersed in water at 60°C: A - no silane primer, B - γ - APS primer at pH 10.4, and C - γ-APS primer at pH 8.0.

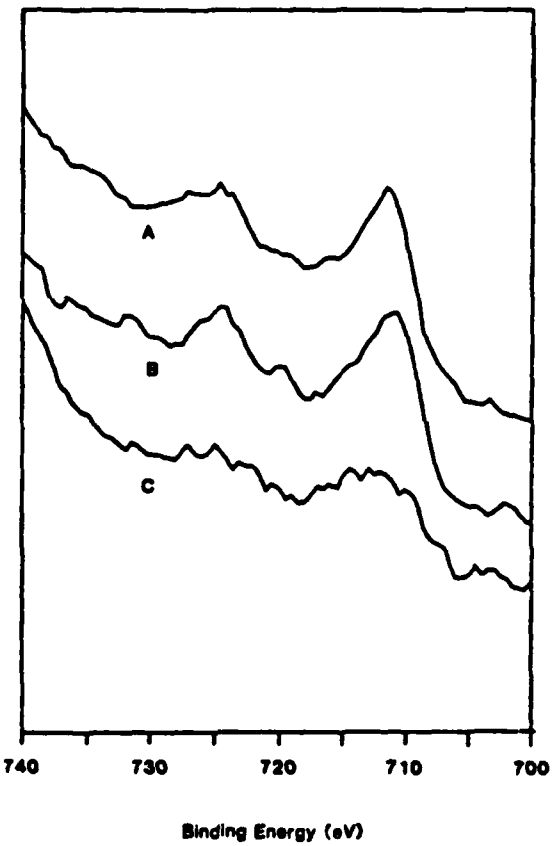

Figure 4. Fe(2p) XPS spectra obtained from adherend fracture surfaces of iron/epoxy lap joints that were tested after 7 days in water at 60°C: A - no silane primer, B - γ-APS primer at pH 10.4, and C - γ-APS primer at pH 8.0.

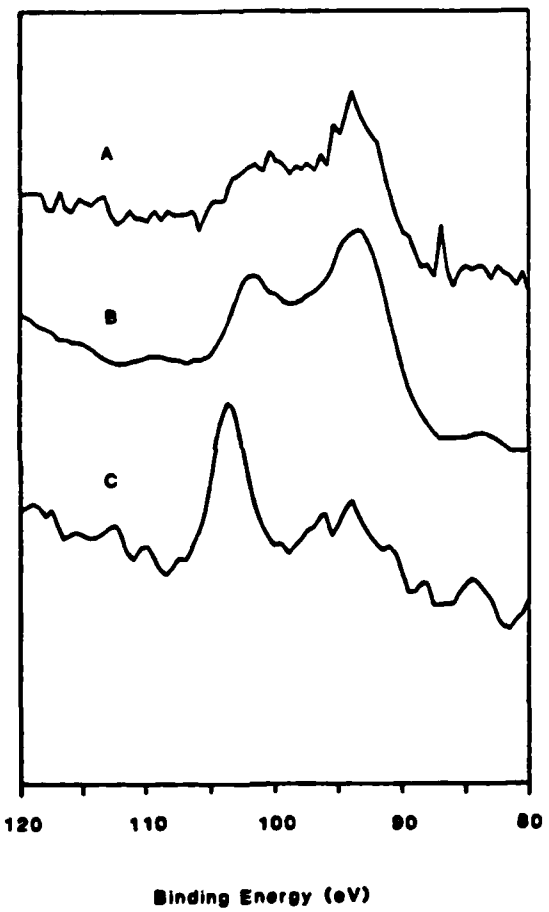

Figure 5. Si(2p) and Fe(3s) XPS spectra obtained from adherend fracture surfaces of iron/epoxy lap joints that were tested after 7 days in water at 60°C: A - no silane primer, B - γ-APS primer at pH 10.4, and C - γ-APS primer at pH 8.0.

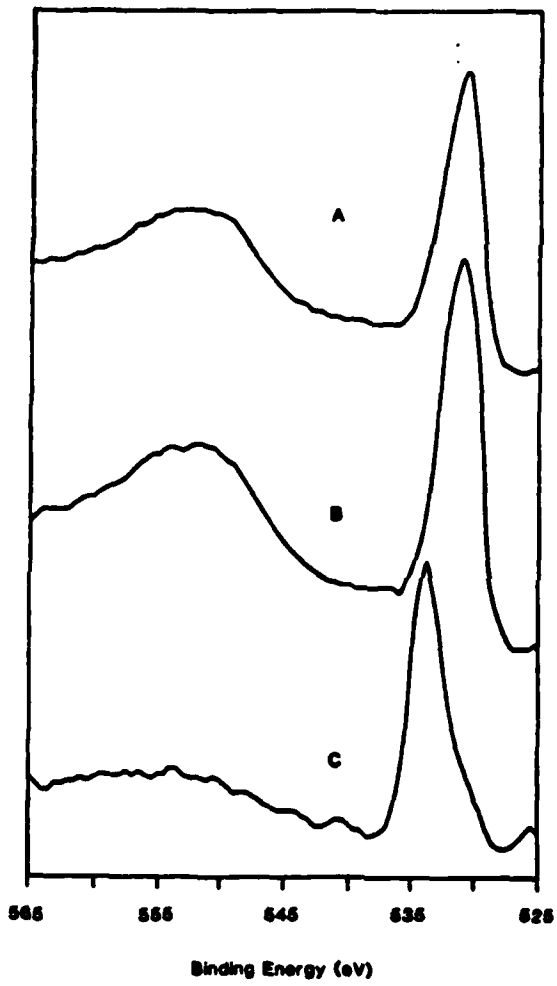

Figure 6. O(1s) XPS spectra obtained from adherend fracture surfaces of iron/epoxy lap joints that were tested after 7 days in water at 60°C: A - no silane primer, B - γ-APS primer at pH 10.4, and C - γ-APS primer at pH 8.0.

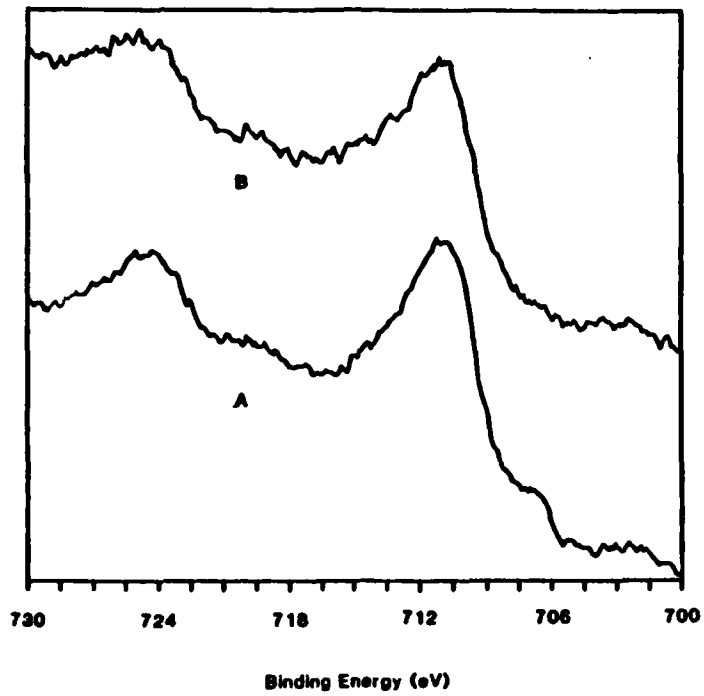

Figure 7. Fe(2p) XPS spectra obtained from mechanically polished iron mirrors. The exit angles were (A) - 90° and (B) - 10°.

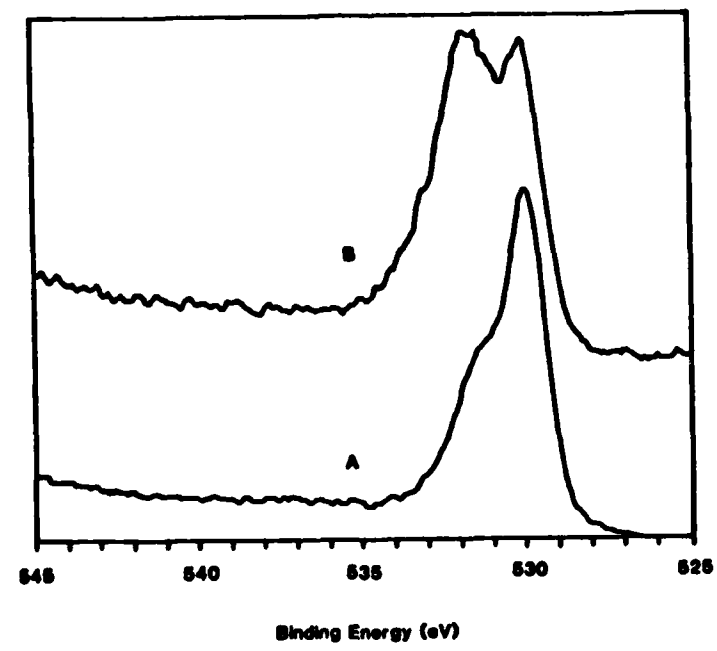

Figure 8. O(1s) XPS spectra obtained from mechanically polished iron mirrors. The exit angles were (A) - 90° and (B) - 10°.

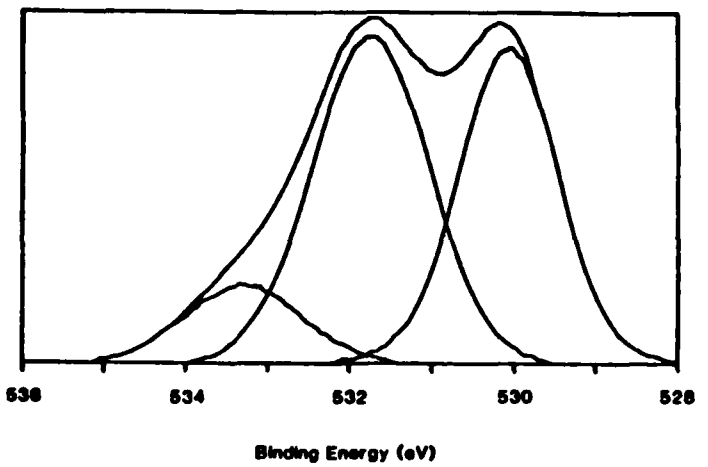

Figure 9. Deconvolution of O(1s) XPS spectra from mechanically polished iron mirrors with exit angle of 10°.

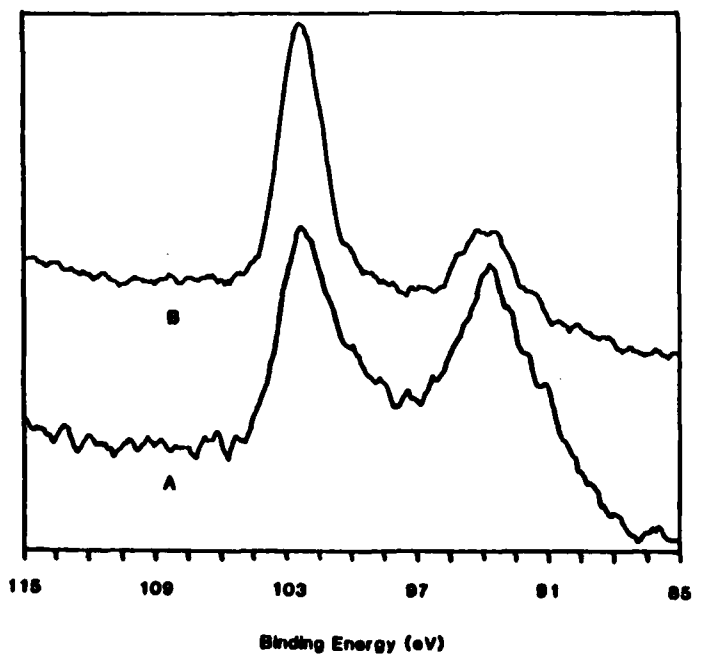

Figure 10. Si(2p) XPS spectra from γ-APS films that were adsorbed onto iron mirrors from 1% aqueous solutions at pH 10.4 and then rinsed. The exit angles were (A) - 90° and (B) - 10°.

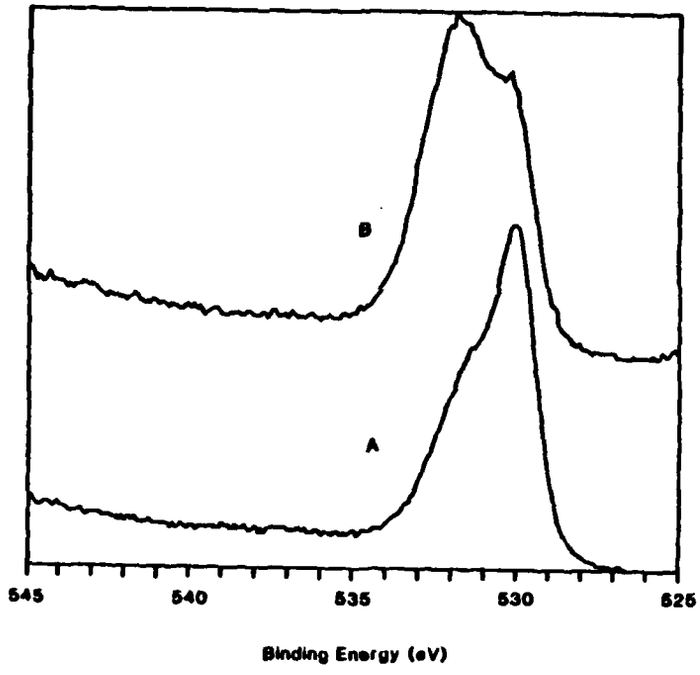

Figure 11. O(1s) XPS spectra from γ-APS films that were adsorbed onto iron mirrors from 1% aqueous solutions at pH 10.4 and then rinsed. The exit angles were (A) - 90° and (B) - 10°.

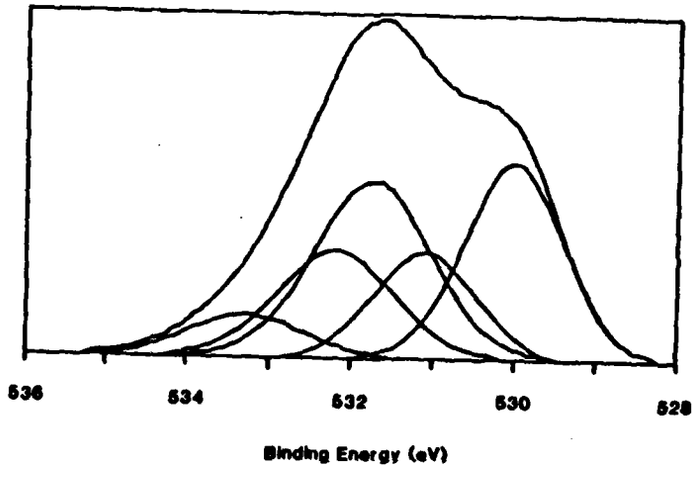

Figure 12. Deconvolution of O(1s) XPS spectra from γ-APS films that were adsorbed onto iron mirrors from 1% aqueous solution at pH 10.4 and then rinsed. The exit angle was 10°.

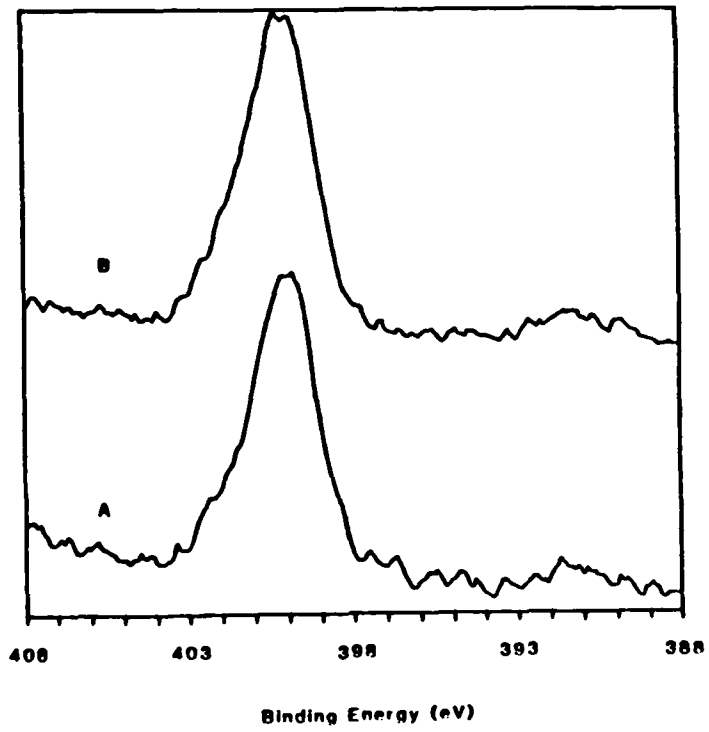

Figure 13. N(1s) XPS spectra from γ-APS films that were adsorbed onto iron mirrors from 1% aqueous solutions at pH 10.4 and then rinsed. The exit angles were (A) - 90° and (B) - 10°.

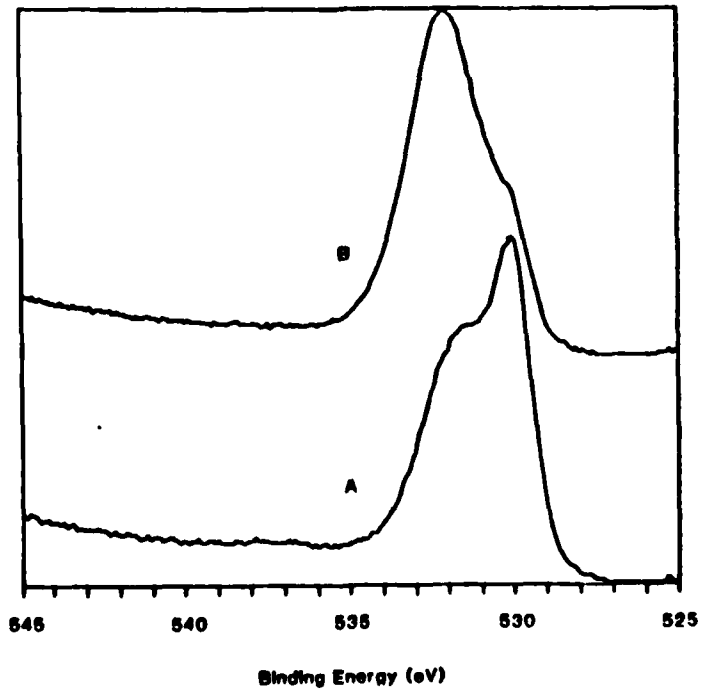

Figure 14. O(1s) XPS spectra from γ-APS films that were adsorbed onto iron mirrors from 1% aqueous solutions at pH 8.0 and then rinsed. The exit angles were (A) - 90° and (B) - 10°.

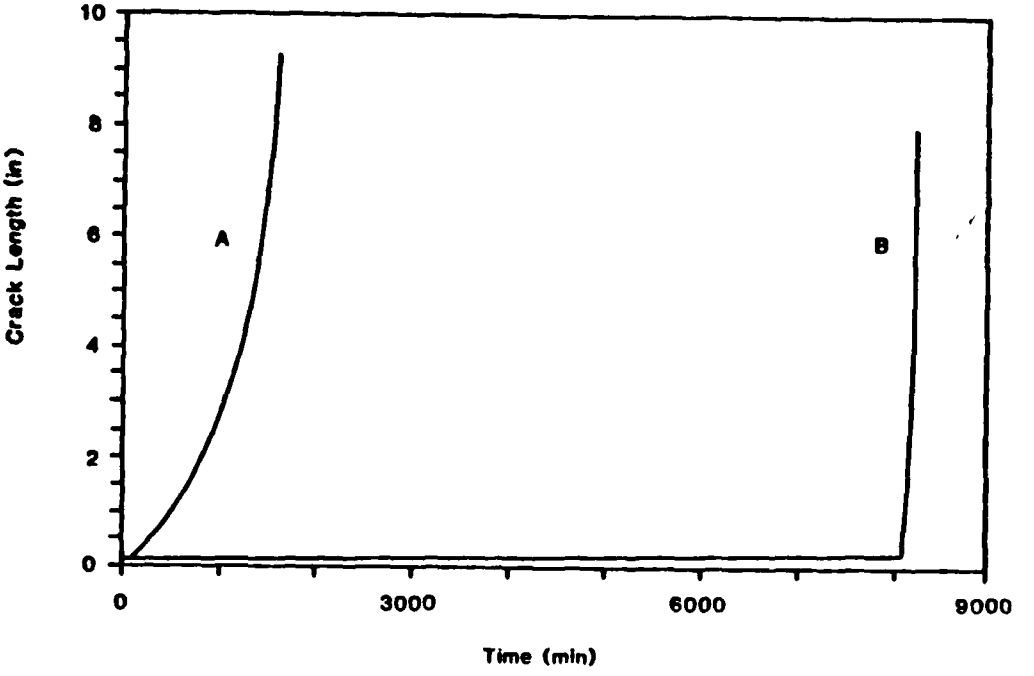

Figure 15. Crack length as a function of time for unprimed aluminum/epoxy TDCB specimens that were statically loaded in water at 60°C. The applied loads were (A) - $G_a = 0.94 \times 10^5$ and (B) - $G_a = 0.85 \times 10^5$ mj/m^2.

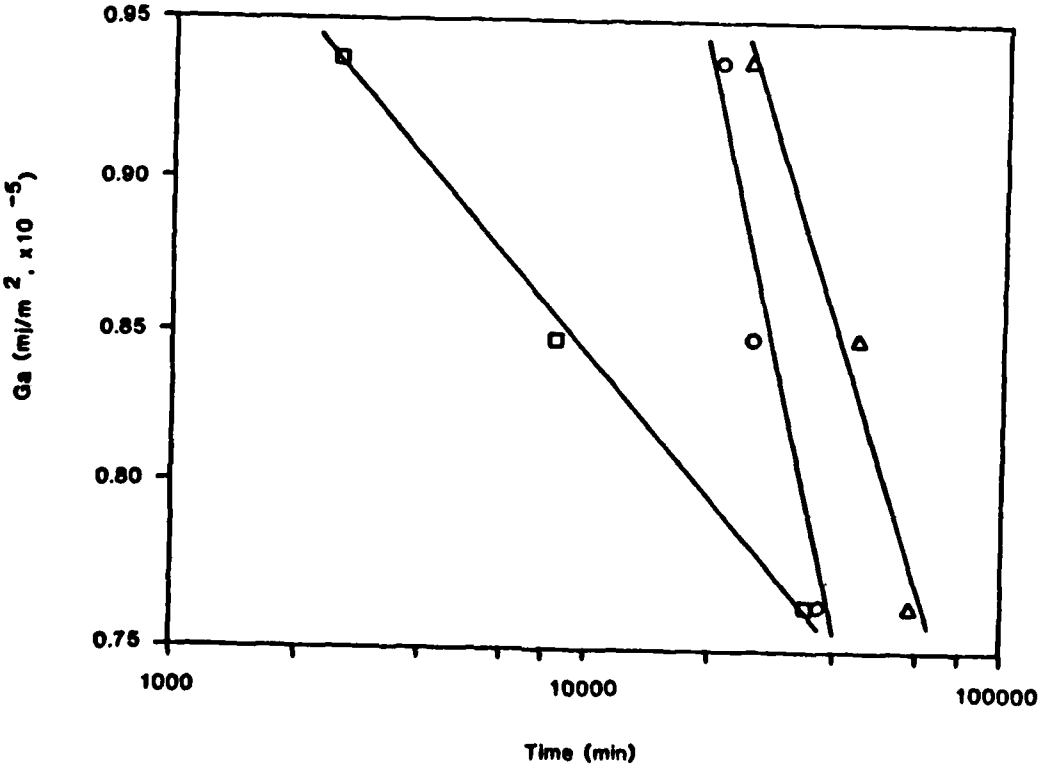

Figure 16. Time to failure as a function of applied load for aluminum/epoxy TDCB specimens immersed in water at 60°C: □ - no silane primer, o - γ-APS primer at pH 10.4, and Δ - γ-APS primer at pH 7.0.

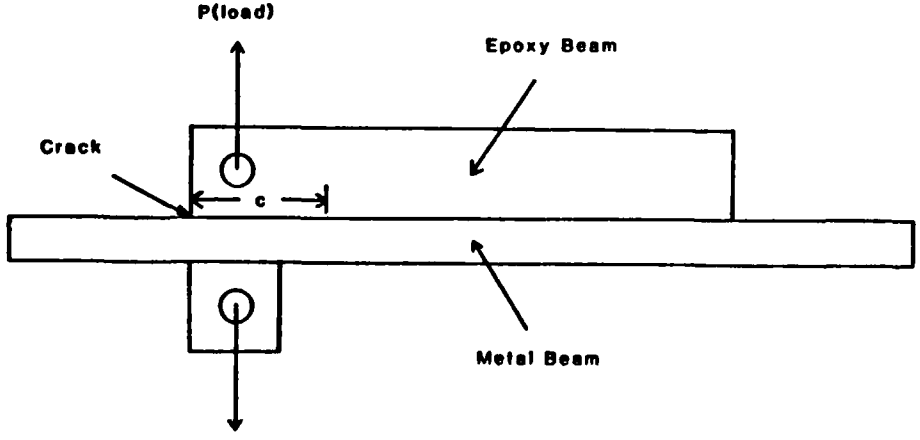

Figure 17. Double cantilever beam specimen for determining effect of residual stresses on durability of adhesive joints.

VI. Publications and Presentations

The following is a summary of publications and papers presented at technical meetings during the preceding year based on work supported by this contract:

A. Publications

"Silane Primers for Improved Hydrothermal Stability of Adhesive Bonds to Aluminum," Proc. ACS Div. Polymeric Mtls. Sci. Engr. 50, 444 (1984).

"Silane Coupling Agents as Hydration Inhibitors for Aluminum Oxides," Proc. 39th Ann. Tech. Coup., SPI Rein. Plastics/Composites Inst., Sec. 1A, 1984.

"Surface Analysis of Silane Primers for Adhesive Bonding of Aluminum Alloys," Proc. Natl. SAMPE Tech. Conf. 1983, 15 (20/20 Vision Mater. 2000), 212-223.

B. Papers Presented at Technical Meetings

"Structure and Properties of Silane Primers for Adhesive Bonding of Iron, Titanium, and Aluminum," presented at Adhesion Principles and Practice for Coating and Polymer Scientists, a short course sponsored by Kent State University, Kent, OH, May 21-25, 1984 (invited).

"Silane Primers for Improved Hydrothermal Stability of Adhesive Bonds to Aluminum," American Chemical Society, St. Louis, MO, April 8-13, 1984.

"Silane Coupling Agents as Hydration Inhibitors for Aluminum Oxides," Society of the Plastics Industry, Houston, TX, January 16-19, 1984.

"Reflection-Absorption Spectroscopy," Pittsburgh Conference, Atlantic City, NJ, March 5-9, 1984 (invited).

"Silane Primers for Improved Hydrothermal Stability of Adhesive Bonds," Virginia Tech Center for Adhesion Science Program Review/Workshop, Blacksburg, VA, April 29 - May 2, 1984.

"Structure and Properties of Silane Primers," Gordon Research Conference on Science of Adhesion, New Hampton, NH, August 22-26, 1983 (invited).

"Surface Analysis of Silane Primers for Adhesive Bonding of Aluminum Alloys," Society for the Advancement of Materials and Process Engineering, Cincinnati, OH, October 4-6, 1983.

ONR Adhesion Science Distribution List

Office of Naval Research (2 copies)
Code 471
800 North Quincy Street
Arlington, VA 22217

Defense Technical Information Center (12 cys)
Building 5, Cameron Station
Alexandria, VA 22314

Dr. L. H. Peebles, Jr.
Office of Naval Research
Code 431
800 North Quincy Street
Arlington, VA 22217

Office of Naval Research
Code 472 (Attn: Dr. K. J. Wynne)
800 North Quincy Street
Arlington, VA 22217

Office of Naval Research
Code 473 (Attn: Dr. R. S. Miller)
800 North Quincy Street
Arlington, VA 22217

Office of Naval Research
Code 474 (Attn: Dr. N. Perrone)
800 North Quincy Street
Arlington, VA 22217

AFOSR
Attn: Dr. D. R. Ulrich, Building 410
Bolling AFB
Washington, DC 20332

AFOSR
Attn: Capt. L. Krebs, Building 410
Bolling AFB
Washington, DC 20332

Naval Research Laboratory
Code 6120 (Attn: Dr. L. Jarvis)
4555 Overlook Avenue, SW
Washington, DC 20375

Naval Air Systems Command
440-JP1 (Attn: Mr. R. Schmidt)
Washington, DC 20361

AFWAL/MLBM (Dr. L. T. Drzal)
WPAFB, OH 45433

AFWAL/MLBM (T. J. Reinhardt)
WPAFB, OH 45433

AFWAL/MLBM (W. B. Jones, Jr.)
WPAFB, OH 45433

AFWAL/MLBM (T. E. Helminiak)
WPAFB, OH 45433

AFWAL/MLBM (I. J. Goldfarb)
WPAFB, OH 45433

AFWAL/MLBM (S. R. Eddy)
WPAFB, OH 45433

AFWAL/MLBM (R. Van Deusen)
WPAFB, OH 45433

NSWC
Attn: Dr. J. Augl
White Oak Laboratory
Silver Spring, MD 20910

NASA Headquarters
Attn: Mr. C. F. Bersch, RTM-6
Washington, DC 20546

NBS
Polymer Science & Studies Division
Attn: Dr. D. L. Hunston
Washington, DC 20234

Army Research Office
Attn: Dr. J. Hurt
P.O. Box 12211
Research Triangle Park, NC 27709

AMMRC
Attn: Dr. N. S. Schneider
Watertown, MA 02172

AMMRC
Attn: Dr. S. E. Wentworth
Watertown, MA 02172

NAVSEA 109CM4
Attn: Mr. H. Vanderveldt
Washington, DC 20362

DTNSRDC-28
Attn: Mr. J. R. Belt
Carderock, MD

Naval Research Laboratory
Code 8433 (Attn: Dr. I. Wolock)
4555 Overlook Avenue, SW
Washington, DC 20375

Naval Weapons Center
Attn: Mr. A. Anster
China Lake, CA 93555

Professor H. Ishida
Dept. of Macromolecular Science
Case Western Reserve University
Cleveland, OH 44106

Professor S. Wang
Dept. of Theoretical & Applied Mechanics
University of Illinois
Urbana, IL 61801

Professor F. J. Boerio
Dept. of Materials Science
University of Cincinnati
Cincinnati, OH 45221

Dr. J. D. Venables
Martin Marietta Laboratories
1450 South Rolling Road
Baltimore, MD 21227

END

FILMED

DTIC